Accurate Reaction Enthalpies and Sources of Error in DFT Thermochemistry for Aldol, Mannich, and α-Aminoxylation Reactions

Steven E. Wheeler, Antonio Moran, Susan N. Pieniazek, and K. N. Houk*

Department of Chemistry and Biochemistry, University of California, Los Angeles, California 90095

Received: June 22, 2009; Revised Manuscript Received: August 3, 2009

Enthalpies for bond-forming reactions that are subject to organocatalysis have been predicted using the high-accuracy CBS-QB3 model chemistry and six DFT functionals. Reaction enthalpies were decomposed into contributions from changes in bonding and other intramolecular effects via the hierarchy of homodesmotic reactions. The order of the reaction exothermicities (aldol < Mannich ≈ α-aminoxylation) arises primarily from changes in formal bond types mediated by contributions from secondary intramolecular interactions. In each of these reaction types, methyl substitution at the β- and γ-positions stabilizes the products relative to the unsubstituted case. The performance of six DFT functionals (B3LYP, B3PW91, B1B95, MPW1PW91, PBE1PBE, and M06-2X), MP2, and SCS-MP2 has been assessed for the prediction of these reaction enthalpies. Even though the PBE1PBE and M06-2X functionals perform well for the aldol and Mannich reactions, errors roughly double when these functionals are applied to the α-aminoxylation reactions. B3PW91 and B1B95, which offer modest accuracy for the aldol and Mannich reactions, yield reliable predictions for the two α-aminoxylation reactions. The excellent performance of the M06-2X and PBE1PBE functionals for aldol and Mannich reactions stems from the cancellation of sizable errors arising from inadequate descriptions of the underlying bond transformations and intramolecular interactions. SCS-MP2/cc-pVTZ performs most consistently across these three classes of reactions, although the reaction exothermicities are systematically underestimated by 1−3 kcal mol^{-1}. Conventional MP2, when paired with the cc-pVTZ basis set, performs somewhat better than SCS-MP2 for some of these reactions, particularly the α-aminoxylations. Finally, the merits of benchmarking DFT functionals for the set of simple chemically meaningful transformations underlying all bond-forming reactions are discussed.

I. Introduction

The field of organocatalysis has experienced dramatic growth in the past decade.[1] Catalysis via organic compounds complements traditional organometallic catalysis and now constitutes a powerful tool in the synthetic armamentarium. In particular, the popularity of proline as a catalyst for asymmetric aldol,[2] Mannich,[3] and α-aminoxylation[4] reactions is a testament to its synthetic utility.[5] Jiang et al.[6] also recently reported the successful de novo computational design of enzymes that catalyze a retro-aldol reaction, providing a glimpse of the potential power of computationally designed enzyme catalysts. These key C−C and C−O bond-forming transformations can provide efficient synthetic routes to valuable chiral compounds. Unfortunately, there is a dearth of reliable experimental enthalpies for these three reaction types. As such, the computational prediction of such thermochemical quantities is vital to fully harness the power of these reactions in synthetic applications, to develop new organocatalytic paradigms, and to design enzyme catalysts for these reactions successfully.

Numerous computational studies utilizing density functional theory (DFT) have explored the mechanisms and origin of stereoselectivity in these reactions[7−10] and even pursued the design of novel catalysts.[11,12] For example, Houk and coworkers[7,8,10] and Boyd and coworkers[9] studied the Hajos−Parrish reaction[13] (a proline-catalyzed asymmetric intramolecular aldol reaction) using the popular B3LYP DFT functional, singling out the operative mechanism from four disparate proposals in the literature[7] and explaining the origin of the stereoselectivity.[8] Subsequent DFT studies have explored the mechanism and stereoselectivity of other reactions catalyzed by proline and proline derivatives.[11] In contrast with these detailed mechanistic explorations of organocatalyzed reactions, accurate studies of the thermochemistry of aldol, Mannich, and α-aminoxylation reactions are lacking.

The field of computational thermochemistry has matured to the point that, for small molecules, it is possible to predict reaction enthalpies to accuracies rivalling the best experiments.[14] In general, this requires the application of computationally demanding composite ab initio approaches.[15] Unfortunately, such rigorous treatments are not currently feasible for larger molecular systems, and thus the employment of more computationally efficient techniques is mandatory. DFT has emerged as a powerful computational tool for the relatively rapid evaluation of reaction enthalpies for large chemical systems.[16] However, because there is no means of systematically improving DFT energies, benchmarking results against robust ab initio data is necessary.[17−19] Recent revelations of systematic errors in DFT energies for seemingly innocuous systems[18,20−22] have prompted a redoubling of efforts to benchmark DFT functionals for the prediction of key classes of organic reactions.[23−25] Development of new DFT functionals to ameliorate some of the underlying issues has also ensued.[19,26,27]

One well-documented deficiency of many DFT functionals is the failure to adequately describe 1,3-alkyl−alkyl interactions (protobranching).[21,22] These interactions, the effect of which is most transparent in the isomerization energies of alkanes, are

* Corresponding author. E-mail: houk@chem.ucla.edu.

10.1021/jp9058565 CCC: $40.75
Published on Web 08/27/2009

vitally important in many reactions. This is particularly true when C−C bonds are formed because the number of protobranching interactions will be unbalanced in such transformations. In addition to protobranching, more general intramolecular effects involving three non-hydrogen-atom fragments (e.g., hyperconjugation and effects arising from the presence of electronegative elements) are created in any bond-forming reaction, and an analysis of the performance of DFT functionals for these interactions is long overdue. Pieniazek, Clemente, and Houk[23] analyzed DFT errors for protobranching, hyperconjugation, conjugation, and $\pi \rightarrow \sigma$ transformations occurring in some C−C bond-forming reactions involving hydrocarbons. The largest deviations from benchmark values arise from the conversion of C−C π-bonds to σ-bonds, an effect attributed to the delocalization errors that plague most DFT functionals.[19,26,28,29] Specifically, reaction enthalpies predicted by popular DFT functionals deviate by almost 9 kcal mol^{-1} from benchmark values for the conversion of acetylene plus two methanes to ethane and ethylene. Errors are almost as large for the reaction of ethylene plus methanes to yield two ethanes.[23]

Any bond-forming reaction will involve changes in the number and types of bonds and three-heavy-atom fragments. By analyzing reaction enthalpies in terms of these changes, we can gain insight into reaction enthalpies across different types of reactions and explain the effects of methylation on enthalpies within a given reaction type. Examination of errors in DFT-predicted enthalpies for basic transformations describing these effects can explain the performance of DFT functionals for aldol, Mannich, and α-aminoxylation reactions and unveil shortcomings of common DFT functionals. A primary aim of this work is to provide accurate enthalpies for reactions that are commonly catalyzed by proline or other catalysts. We also seek to explain trends in enthalpies for these reactions and to assess errors in DFT predictions for these reaction enthalpies and their underlying components. The results will guide computational chemists in choosing appropriate theoretical methods from the ever-growing DFT menagerie for mechanistic studies of organanocatalytic reactions and the design of novel catalysts.[12]

II. Theoretical Methods

Accurate reaction enthalpies (0 K) were computed using the CBS-QB3 model chemistry.[30] This composite approach combines a series of ab initio energy evaluations with basis set extrapolations to deliver an estimate of the complete basis set limit CCSD(T) energy. Previous benchmarks[30,31] have demonstrated that this method delivers reaction enthalpies typically within 1 to 2 kcal mol^{-1} of experiment for a range of bond-forming transformations, although for cases involving unbalanced multireference character such "black-box" approaches can yield less-reliable thermochemical predictions.[32] CBS-QB3 has been shown to be generally reliable for basic bond separation energetics. For the α-aminoxylation reactions, enthalpies were also computed with the G3 model chemistry[33] to confirm CBS-QB3 results. The largest deviation between G3 and CBS-QB3 was 0.3 kcal mol^{-1}. Because experimental enthalpies are available for only one of the target reactions, CBS-QB3 data are used as benchmark results and form the basis of evaluation of DFT and other theoretical approaches. For some of the molecules considered, there are multiple low-lying conformations. We consider only the lowest-lying gas-phase conformation and report enthalpies at 0 K. Consequently, direct comparison with experiments, which will reflect a Boltzmann distribution of conformations, should be done mindfully.

Six DFT functionals were tested: five hybrid GGAs (B3LYP,[34,35] B3PW91,[34,36] B1B95,[37] MPW1PW91,[36,38] and PBE1PBE[39]) and the hybrid meta-GGA M06-2X.[40] For each of these functionals, geometries were optimized and harmonic vibrational frequencies were computed using the 6-31+G(d,p) and 6-311+G(2df,2p) basis sets. Results are presented primarily using the triple-ζ quality 6-311+G(2df,2p) basis set. 6-31+G(d,p) data are tabulated in the Supporting Information. For comparison, results from second-order Møller−Plesset perturbation theory (MP2) and the spin-component scaled analogue (SCS-MP2)[41] are also included, computed using the cc-pVTZ basis set.[42] This latter approach has been shown to be a computationally efficient yet robust approach for general organic reactions.[43] SCS-MP2/cc-pVTZ reaction enthalpies arise from single-point energies evaluated at MP2/cc-pVTZ optimized geometries, appended with zero-point vibrational energy corrections from unscaled MP2/cc-pVTZ frequencies. To discern the effects of basis-set size, MP2/cc-pVDZ and SCS-MP2/cc-pVDZ enthalpies are included in the Supporting Information. DFT integration grids with 70 radial and 590 angular points were utilized in all M06-2X computations, which were executed with NWChem 5.1.[44] Gaussian 03 was used for the other computations.[45]

III. Results and Discussion

A. Enthalpies for Aldol, Mannich, and α-Aminoxylation Reactions. Representative aldol (1−4), Mannich (5−7), and α-aminoxylation (8 and 9) reactions are listed in Scheme 1, along with CBS-QB3 predicted reaction enthalpies. In the aldol reactions, a C═O bond is replaced by C−C and C−O bonds, whereas the Mannich reactions involve a conversion of a C═N bond into C−C and C−N bonds. A N═O bond is replaced by C−O and N−O bonds in the α-aminoxylation reactions. Within each type of reaction, methyl groups have been introduced in the reactants to study the effects of branching on the thermochemistry of these transformations. Among these reactions, it is only possible to evaluate the enthalpy of reaction 4 from tabulated experimental enthalpies of formation.[46] In this case, CBS-QB3 performs well, falling about 1 kcal mol^{-1} from the experimental upper bound.

Reactions 1−9 are all predicted to be exothermic, with predicted ΔH_{0K} values ranging from −9.2 to −21.1 kcal mol^{-1}. In general, the α-aminoxylation reactions (8 and 9) are the most exothermic, and the aldol reactions (1−4) are the least exothermic. It should be noted that the Gibbs free energies for these bimolecular reactions are less negative than the reaction enthalpies. For example, the predicted Gibbs free energy for reaction 4 is +3.2 kcal mol^{-1} at 298 K, which is consistent with the favorable retro-aldol decomposition of 4-hydroxy-4-methylpentan-2-one to yield acetone.[47]

In the crudest approximation, the enthalpy of a given reaction arises from changes in formal bond types. Isogyric[48] reactions 10−12 (Scheme 2) quantify the changes in bonding that occur in the aldol, Mannich, and α-aminoxylation reactions, respectively. For example, reaction 10 is the simplest reaction that captures the bonding changes that occur during the aldol reaction. In both the aldol and reaction 10, there is a net conversion of C═O and C−H bonds in the reactants into C−O, C−C, and O−H bonds in the products. Reactions 11 and 12 similarly depict the bonding changes that occur in the Mannich and α-aminoxylation reactions, respectively. CBS-QB3 enthalpies are provided for each of these reactions, along with available experimental results. Clearly, consideration of changes in bonding alone is insufficient to explain the exothermicities of reactions 1−9.

Additional contributions to reaction enthalpies arise from changes in intramolecular interactions, including hyperconju-

SCHEME 1: CBS-QB3 Enthalpies (ΔH_{0K}, in kcal mol^{-1}) for Aldol (1−4), Mannich (5−7), and α-Aminoxylation (8 and 9) Reactions[a]

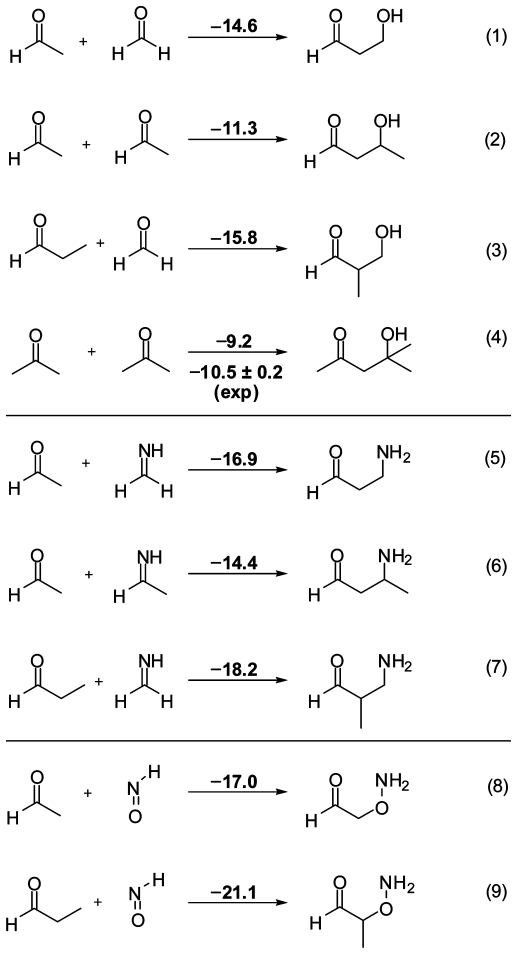

[a] Experimental enthalpy for reaction 4 was calculated from NIST enthalpies of formation for the reactants and products.[46]

SCHEME 2: Isogyric Reactions Representing the Changes in Bonding in the Aldol, Mannich, and α-Aminoxylation Reactions[a]

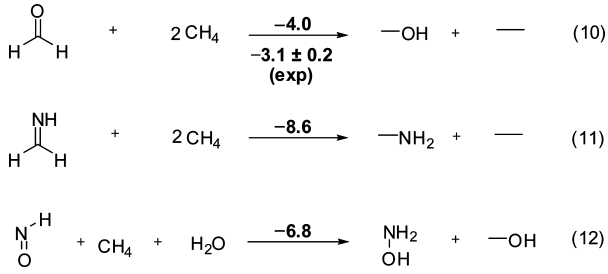

[a] Enthalpies of reaction (ΔH_{0K}, kcal mol^{-1}) computed at the CBS-QB3 level.

gation, protobranching, and various effects arising from alkyl groups bonded to heteroatomic centers as well as longer-range effects. These sundry effects can be quantified using isodesmic,[49] homodesmotic,[50,51] and hyperhomodesmotic[51,52] transformations. Consequently, reactions 1, 5, and 8 can each be written as a sum of four reactions, with each successive reaction capturing the effects of longer-range intramolecular effects. This is demonstrated for reaction 1 in Scheme 3. Analogous decompositions for reactions 5 and 8 are provided in Schemes S1 and S2 of the Supporting Information. These model reactions decompose the given reaction enthalpy into contributions due to changes in bonding (the isogyric reaction) and intramolecular effects involving three (the isodesmic reaction), four (the homodesmotic reaction), and five (the hyperhomodesmotic reaction) non-hydrogen-atom fragments. This follows from the definition of the *n*-homodesmotic hierarchy,[51] in which main chains of length *n* are conserved ($n = 2$, isodesmic; $n = 3$, homodesmotic; $n = 4$, hyperhomodesmotic, etc.). The resulting decompositions of the enthalpies for reactions 1, 5, and 8 are listed in Table 1, all evaluated using CBS-QB3.

In this way, the different contributions to the total reaction enthalpy due to changes in the molecular environment going from reactants to products can be quantified. In the case of aldol and α-aminoxylation reactions 1 and 8, the contribution to the total reaction enthalpy from changes in bonds is smaller than the contribution from unbalanced three-heavy-atom interactions (protobranching, hyperconjugation, etc.). The decomposition of the enthalpy of Mannich reaction 5 reveals similar stabilizing effects due to unbalanced three-atom interactions, but in this case, these are outweighed by the effects of changes in formal bond types. For each of these reactions, the contributions from four-atom fragments are significantly smaller than those from the three-atom components, as expected. However, the magnitudes of the five-atom interactions remain significant because of the effects of intramolecular hydrogen bonding.

B. Effect of Methyl Substitution on Reaction Enthalpies. The effect of methyl substitution on the enthalpies of reactions 1, 5, and 8 has been explored. Reactions 1 and 5 are more exothermic than reactions 2 and 6, despite the higher degree of branching in the products of the latter two reactions. This is due to compensating stabilizing intramolecular interactions in the reactants. Isodesmic[48,51] bond separation reactions 16−21 (Scheme 4) quantify the enthalpic benefit of attaching a methyl group to ethane, methanol, methylamine, hydroxylamine, formaldehyde, and methanimine, respectively. The effects responsible for this stabilization include protobranching and hyperconjugation, among others. Together, these effects explain the observed magnitudes of the exothermicities within each reaction type. For aldol reaction 1, the propane-like (C−C−C) and ethanol-like (C−C−O) interactions present in the products but not the reactants (16 + 17) contribute $-3.0 + (-5.8) = -8.8$ kcal mol^{-1} to the overall reaction enthalpy of −14.6 kcal mol^{-1}.[53] Reaction 2 has two of each of these interactions present in the products that are not balanced in the reactants, contributing an additional −8.8 kcal mol^{-1}. However, the hyperconjugative interaction between alkyl group and a carbonyl (reaction 20) in the reactants not present in the products offsets these stabilizing interactions, raising the reaction enthalpy by 11.1 kcal mol^{-1}. Therefore, $11.1 + (-8.8) = 2.2$ kcal mol^{-1} of the 3.4 kcal mol^{-1} difference between the enthalpies of reactions 2 and 1 is accounted for by unbalanced interactions in these three-atom fragments. The remaining 1.1 kcal mol^{-1} presumably comes mostly from longer-range effects. Similarly, the low exothermicity of reaction 4 compared with that of 1 arises from the hyperconjugative interactions in the reactants overshadowing the alkyl−alkyl and alkyl−hydroxyl interactions in the products of reaction 4. The enthalpy differences among the other reactions of each type can similarly be understood in terms of changes in these interactions involving three-atom fragments. Consequently, theoretical approaches that accurately predict the enthalpies of bond transformation reactions 10−12 as well as isodesmic bond separation reactions 16−21 should reliably predict enthalpies of reactions 1−9. We will see below, however, that the converse, in general, is not true; many DFT functionals

SCHEME 3: Decomposition of Aldol Reaction 1 into a Sum of Isogyric (10), Isodesmic (13), Homodesmotic (14), and Hyperhomodesmotic (15) Reaction Enthalpies (ΔH_{0K}, kcal mol^{-1})[a]

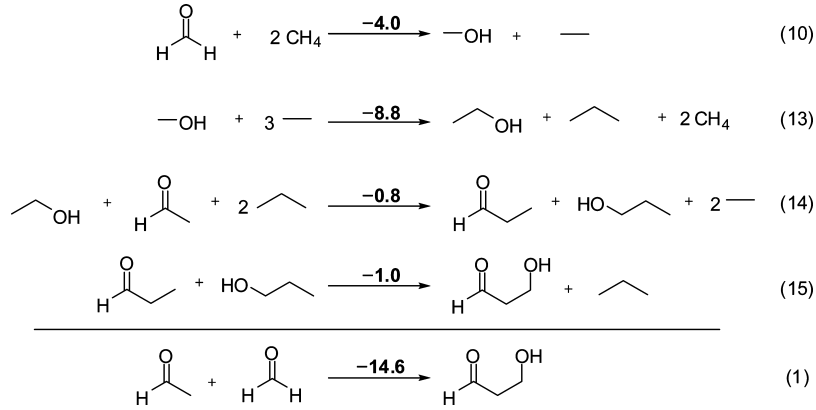

[a] These reactions quantify the effects of unbalanced bonding and intramolecular effects involving three-, four-, and five-atom fragments in reaction 1.

TABLE 1: Reaction Enthalpies (ΔH_{0K}, in kcal mol^{-1}) and Contribution to the Reaction Enthalpies from Changes in Bonds, Three-, Four-, and Five-Heavy-Atom Fragments for the Simplest Aldol, Mannich, and α-Aminoxylation Reactions

		bonds	three-atom fragments	four-atom fragments	five-atom fragments[a]	ΔH_{0K}
aldol	(1)	−4.0	−8.8	−0.8	−1.0	−14.6
mannich	(5)	−8.6	−7.7	−0.5	−0.2	−16.9
α-aminoxylation	(8)	−6.8	−12.2	−0.6	2.5	−17.0

[a] Large contributions from five-atom fragments are due to intramolecular hydrogen bonds.

SCHEME 4: Isodesmic Bond Separation Reactions That Quantify the Three-Heavy-Atom Intramolecular Interactions Present in Reactions 1−9[a]

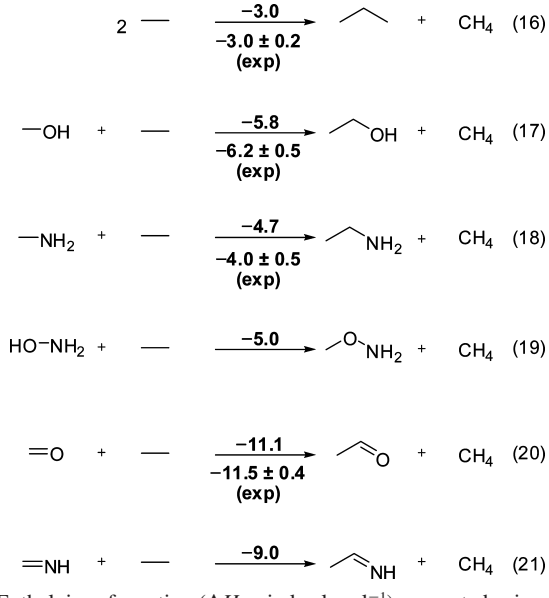

[a] Enthalpies of reaction (ΔH_{0K}, in kcal mol^{-1}) computed using CBS-QB3. Experimental enthalpies (below arrows) computed from NIST enthalpies of formation.[46]

that yield accurate enthalpies for reactions 1−9 actually perform poorly when applied to the simple underlying transformations.

To clarify the effects of methyl substitution on the enthalpies of aldol, Mannich, and α-aminoxylation reactions, thermochemical networks of isodesmic reactions are presented in Scheme 5. These sets of reactions show the enthalpic relationship between methylated and unmethylated reactants and products of reactions 1−9 (which appear as vertical arrows in Scheme 5). For example, this reaction network offers an alternative demonstration of the origin of the relatively low exothermicity of reaction 2 compared with that of reaction 1. The fact that **A** → **D** (reaction 1) in Scheme 5a is 3.3 kcal mol^{-1} more exothermic than **C** → **F** (reaction 2) is due to the **A** → **C** reaction enthalpy of −11.1 kcal mol^{-1}. Indeed, for each of the three reaction classes, the relative enthalpic stability of the products with respect to the unsubstituted reactants plus ethane as a common starting point (**A**, in boxes) follows the expected order based on the stabilizing three-heavy-atom effects quantified in reactions 16−21. The products substituted at the γ-position are more stable than those substituted at the β-position. This is due to the greater stabilization afforded by the ethanol- and ethanamine-like fragments in the γ-substituted products compared with the corresponding propane-like fragment in the β-substituted product. Both substituted products are more stable than the unsubstituted product, relative to **A**.

C. Sources of Error in DFT, MP2, and SCS-MP2 Predicted Thermochemistry. Errors in DFT, MP2, and SCS-MP2 predicted enthalpies for reactions 1−9 are assessed on the basis of the CBS-QB3 data provided in Scheme 1. For each reaction type (aldol, Mannich, and α-aminoxylation), mean absolute deviations, mean errors, and error ranges for each method are plotted in Figure 1. The 6-311+G(2df,2p) basis set was used. Details for each reaction are provided in the Supporting Information, along with results computed with double-ζ basis sets.

Errors for the aldol and Mannich reactions follow similar trends; B3LYP exhibits the largest errors, followed by B3PW91 and B1B95. PBE1PBE, MPW1PW91, M06-2X, and SCS-MP2 offer more reliable predicted enthalpies, with mean errors of about 2 kcal mol^{-1}. The spread of MPW1PW91 errors, however, is large, ranging from −1.1 to +5.8 kcal mol^{-1}. Even though the distribution of errors for SCS-MP2 is small, this approach systematically underestimates the exothermicity of these two classes of reactions compared with CBS-QB3. For the two α-aminoxylation reactions, the outcome is similar; SCS-MP2 predicts reaction enthalpies that are consistently 3 kcal mol^{-1} less exothermic than the CBS-QB3 values. For the aldol and α-aminoxylation reactions, conventional MP2 yields reaction enthalpies that are in better agreement with CBS-QB3, whereas for the Mannich reactions, SCS-MP2 offers a slight improvement over MP2.

SCHEME 5: Enthalpies of Reaction (ΔH_{0K}, kcal mol^{-1}) at the CBS-QB3 Level of Theory for Isodesmic Reactions Relating the Substituted and Unsubstituted (a) Aldol, (b) Mannich, and (c) α-Aminoxylation Reactants and Products[a]

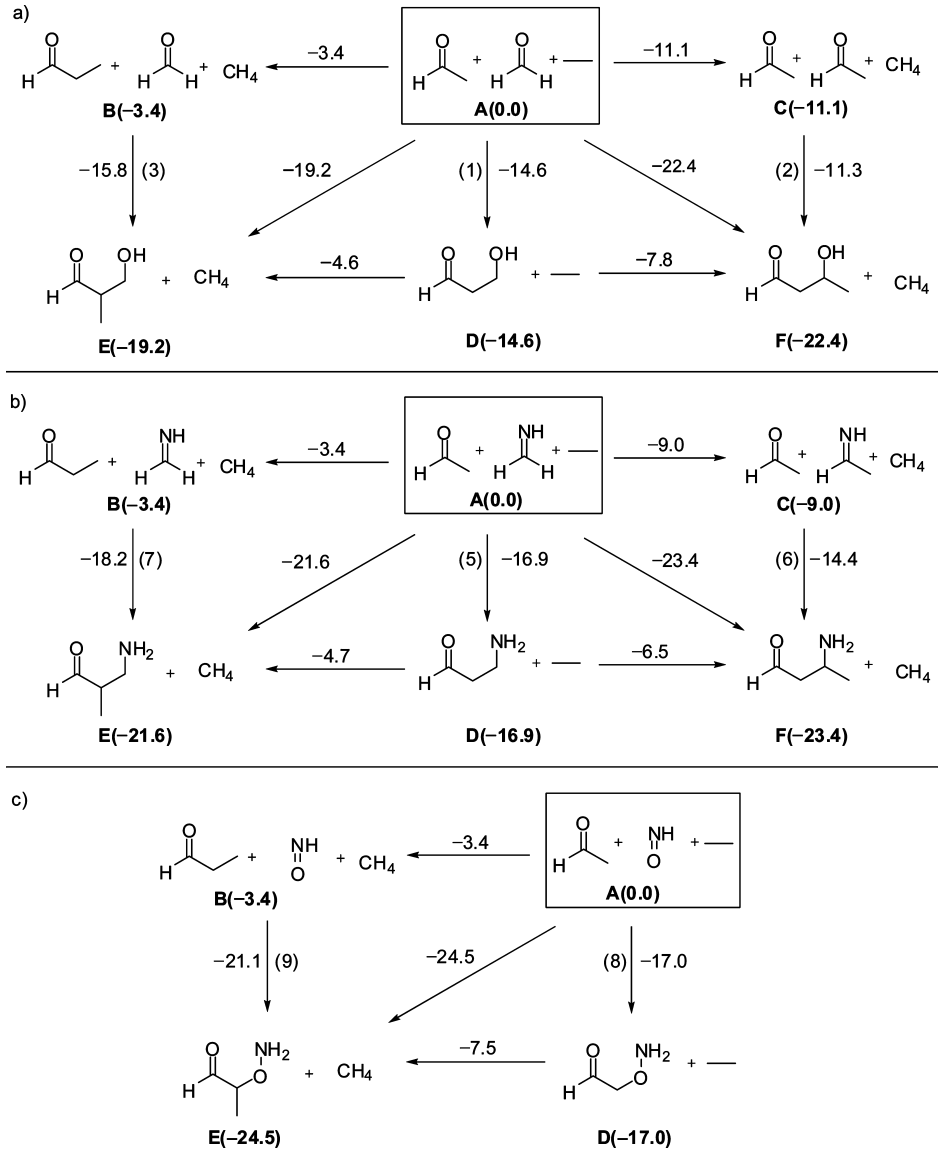

[a] Unsubstituted reactants (**A**), β-substituted reactants (**B**), α-substituted reactants (**C**), unsubstituted products (**D**), β-substituted products (**E**), and γ-substituted products (**F**). Enthalpies of species **B**−**F** are given relative to the unsubstituted reactants (**A**).

The performance of the DFT functionals is qualitatively different for the α-aminoxylation reactions than for the two types of C−C bond-forming reactions. The best-performing functionals for the aldol and Mannich reactions (M06-2X and PBE1PBE) yield much larger errors for the α-aminoxylation reactions. Moreover, B3LYP, which predicted aldol and Mannich reaction enthalpies between 5 and 10 kcal mol^{-1} less exothermic than the benchmark values, performs satisfactorily when applied to the α-aminoxylation reactions. Similarly, the errors from the B3PW91 and B1B95 functionals for the α-aminoxylation reactions are a fraction of those observed for the aldol and Mannich. These results highlight a well-known pitfall in applications of DFT; a given functional can perform well for one type of reaction yet yield erroneous predictions for seemingly similar transformations.

For applications of DFT to large chemical systems, it is customary to employ small basis sets, such as 6-31+G(d,p), for practical purposes. Comparing the 6-311+G(2df,2p) results with those from the polarized double-ζ-quality 6-31+G(d,p) basis set (see Table S2 in the Supporting Information), we see modest basis set effects for the DFT methods. In accord with the results of Pieniazek et al.,[23] the use of the triple-ζ basis set decreases the DFT-predicted exothermicities compared with the 6-31+G(d,p) results in these cases by about 1 kcal mol^{-1}. Consequently, for three of the functionals (B3LYP, B3PW91, B1B95), the use of the larger basis set actually leads to a worse agreement with the CBS-QB3 results. For M06-2X and PBE1PBE, the use of 6-311+G(2df,2p) instead of 6-31+G(d,p) moves the predicted enthalpies closer to the benchmark values. MPW1PW91 exhibits less regular behavior. The accuracy for the Mannich and α-aminoxylation reactions improves with the use of the larger basis, whereas the aldol predictions worsen. As expected, the MP2 and SCS-MP2 results are greatly improved with the use of a triple-ζ basis set compared with cc-pVDZ results.

For most of the DFT functionals studied, the errors for reactions 1−9 (Scheme 1) increase with increasing substitution of the reactant. This is demonstrated in Figure 2, where errors relative to CBS-QB3 are plotted for reactions 1−4. The degree of branching increases across this series of reactions. The

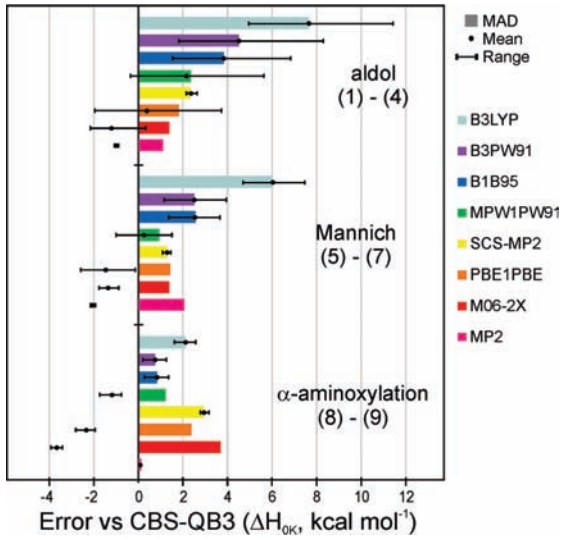

Figure 1. Mean absolute deviation (MAD), mean, and error ranges in predicted aldol, Mannich, and α-aminoxylation reaction enthalpies (ΔH_{0K}, in kcal mol^{-1}) with respect to CBS-QB3. 6-311+G (2df,2p) basis set used for all computations.

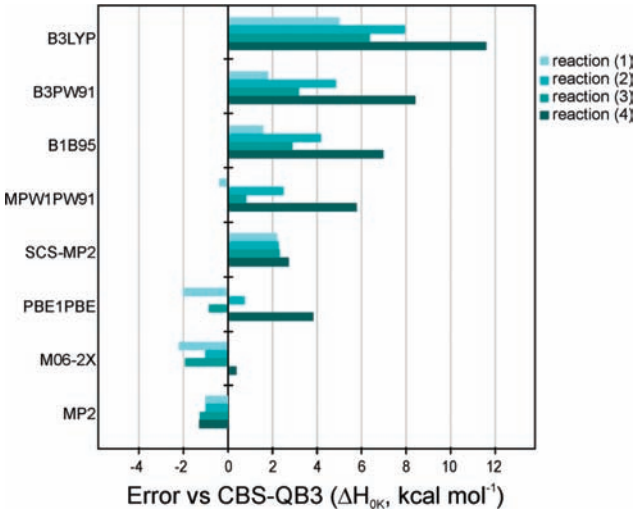

Figure 2. Comparison of errors (kcal mol^{-1}) for aldol reactions 1−4, showing that for most methods, the errors increase with increasing methyl substitution.

observed error increases are partially due to previously documented[21,22] deficiencies of many DFT functionals to account for branching. The M06-2X functional actually performs better for the more highly substituted systems, suggesting that there is some error compensation at play. The MP2 and SCS-MP2 results are insensitive to the degree of branching, and this approach performs consistently across reactions 1−4.

These findings can be understood by examining errors for isodesmic bond separation reactions 16−21 (Scheme 3). These errors are plotted in Figure 3. Reaction 16 is the defining reaction for protobranching, for which errors in popular DFT have previously been discussed.[18,21,22,25] DFT errors for the stabilizing interactions in the other three-atom fragments are of a similar magnitude, all hovering around ±1 kcal mol^{-1}. The M06-2X functional offers the most satisfactory description of these reactions. SCS-MP2, which exhibits very small errors for reactions 16−18, predicts enthalpies with much larger errors for reactions 19−21 compared with CBS-QB3. For reactions 17−19 and 21, SCS-MP2 represents an improvement over MP2, whereas the SCS-MP2 datum for reaction 16 is slightly worse

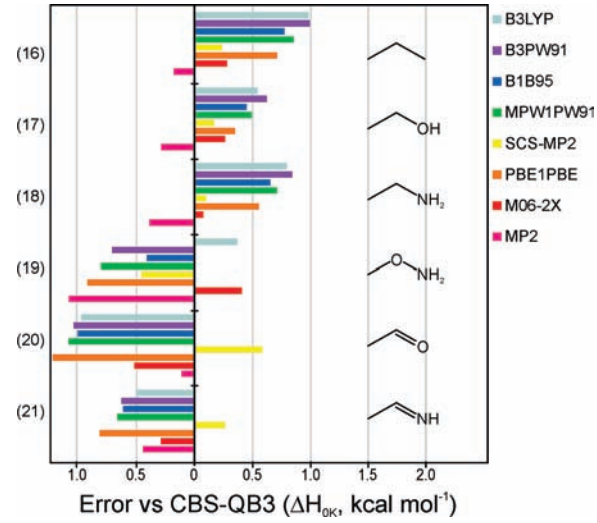

Figure 3. Comparison of errors (kcal mol^{-1}) of different methods with respect to CBS-QB3 for reactions 16−21. These reactions quantify the enthalpic stabilization that is inherent in the three-atom fragments that change during aldol, Mannich, and α-aminoxylation reactions 1−9.

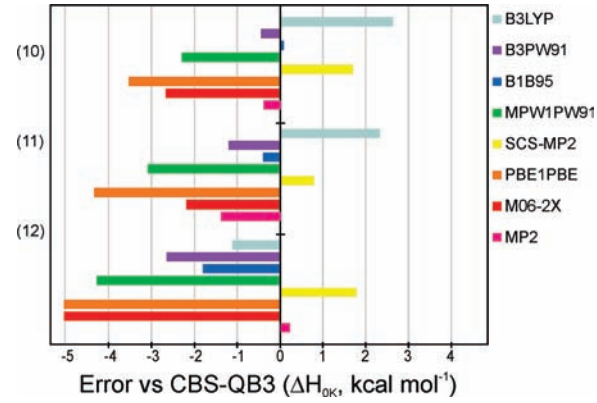

Figure 4. Comparison of errors (kcal mol^{-1}) of different methods with respect to CBS-QB3 for reactions 10−12 (Scheme 2). These reactions quantify the bond transformations present in aldol, Mannich, and α-aminoxylation reactions, respectively.

than the MP2 value. For reaction 20, MP2 performs significantly better than SCS-MP2, which differs from the CBS-QB3 benchmark by 0.6 kcal mol^{-1}. M06-2X is the only DFT functional that predicts the enthalpy of reaction 20 within 0.5 kcal mol^{-1} of the CBS-QB3 result.

Errors in predicted enthalpies for reactions 10−12 (Scheme 2) are plotted in Figure 4 to further dissect the deviations from the CBS-QB3 results for reactions 1−9. Recall that reactions 10, 11, and 12 (Scheme 2) capture the π-to-σ bond changes that occur during aldol, Mannich, and α-aminoxylation reactions, respectively. The MP2 error for reaction 12 is only 0.2 kcal mol^{-1}, underlying the excellent performance of MP2 for the α-aminoxylation reactions in Scheme 1. The performance of the various DFT functionals for these basic transformations is contrary to that observed for reactions 1−9. Even though B3PW91 was among the worst performers for reactions 1−9, it is one of the more accurate functionals for the underlying bond transformations. Similarly, despite providing accurate predicted enthalpies for reactions 1−9, the PBE1PBE and M06-2X functionals perform relatively poorly for reactions 10−12. This parallels the findings of Pieniazek et al.[23] These errors for $\pi \rightarrow \sigma$ transformations are typically attributed to delocalization errors with many DFT functionals.[19,26,28,29] Perhaps most importantly, the DFT errors for the $\pi \rightarrow \sigma$ transformations in

reactions 10−12 are significantly larger than those arising for isodesmic bond separation reactions 16−21 (Scheme 4). This underlies long-known performance enhancements observed when using isodesmic reactions for computational thermochemistry; balancing formal bond types typically yields a greater increase in error cancellation than subsequently balancing three-atom fragments.[48,51,54] Of course, in many applications, the number of unbalanced three-atom fragments often exceeds unbalanced bond types, and thus both sources of error are potentially significant.

Together, these DFT errors are initially confounding. Some functionals that perform well for reactions 1−9 provide lackluster results when applied to the underlying bond transformations. This results from the cancellation of errors in applications to reactions 1−9, which of course is not new for DFT functionals.[23,55] For example, the M06-2X enthalpy for reaction 4 lies only 0.4 kcal mol^{-1} from the CBS-QB3 value of −9.2 kcal mol^{-1}. This is within the error bars of CBS-QB3. However, the M06-2X error for the underlying $\pi \rightarrow \sigma$ bond change (reaction 10) is significantly larger (−2.7 kcal mol^{-1}). This sizable error is compensated for by errors in the intramolecular interactions quantified in Scheme 4. The unbalanced three-atom fragments in reaction 4 are the two acetaldehyde-like groups in the reactants and four propane and three ethanol-like fragments in the products. The former contributes an error of +0.5 kcal mol^{-1} to the M06-2X error for reaction 4, whereas the latter two effects together contribute +2.1 kcal mol^{-1}. Therefore, the total error due to unbalanced three-atom fragments is +2.6, which cancels the bond-transformation error of −2.7 kcal mol^{-1}. The remaining 0.5 kcal mol^{-1} of the error can be attributed to longer-range effects. Similarly, the functionals that perform poorly for reactions 1−9 do so largely because these errors combine constructively. For example, the fact that the B3LYP error for reaction 10 is positive spoils any cancellation with the errors due to three-atom fragments. In reaction 4, imbalances in three-heavy-atom interactions contribute an error of +6.5 kcal mol^{-1}, which, when combined with the error of +2.6 kcal mol^{-1} for the bond changes, account for 9.1 kcal mol^{-1} of the 11.6 kcal mol^{-1} difference between the B3LYP and CBS-QB3 results.

IV. Summary and Concluding Remarks

Accurate thermochemical data have been computed using the CBS-QB3 model chemistry for a series of synthetically useful C−C and C−O bond-forming transformations that can be catalyzed by proline and other common catalysts. A scheme is presented by which reaction enthalpies can be decomposed into contributions from changes in bonds and larger molecular fragments via the *n*-homodesmotic hierarchy.[51] Using these decompositions, it has been shown that intramolecular interactions involving three heavy atom fragments (e.g., protobranching, hyperconjugation, and heteroatomic effects) have a significant impact on the enthalpy of these reactions. In the case of the simplest aldol and α-aminoxylation reactions, the effect of these interactions exceeds that from the forming and breaking of bonds. The overall order of exothermicities (aldol < Mannich ≈ α-aminoxylation) arises from the competing effects of bonding changes and differential intramolecular interactions. Imbalances in these interactions also explain the effect of methyl substitution on the enthalpies of these reactions.

For the aldol and Mannich reactions, the PBE1PBE, MPW1PW91, and M06-2X functionals and the MP2 and SCS-MP2 methods all predict enthalpies with mean errors of about 2 kcal mol^{-1}. B3LYP, B3PW91, and B1B95 perform more poorly for these reactions, with errors as large as 11.6 kcal mol^{-1}. For the α-aminoxylation reactions, this performance is mostly reversed and the B3PW91, B1B95, and MPW1PW91 functionals offer the best performance among the functionals considered. The MPW1PW91 is the only DFT functional to predict reaction enthalpies on average within about 2 kcal mol^{-1} for all three classes of reactions, although with a large spread in errors. For the underlying changes in formal bond types (reactions 10−13), the performance of DFT functionals is actually different than that observed for reactions 1−9 (Scheme 1). Functionals such as M06-2X and PBE1PBE that excelled when applied to reactions 1−9 predict enthalpies for the underlying $\pi \rightarrow \sigma$ bond transformations in error by up to 5 kcal mol^{-1}. The excellent performance of these functionals for reactions 1−9 stems from the cancellation of more sizable errors. Errors for general intramolecular interactions in three-atom fragments parallel those from protobranching interactions.[21,25] Because of the additivity of such errors, for highly branched systems, these errors can become significant. SCS-MP2/cc-pVTZ, which accurately predicts bond separation enthalpies for propane, ethanol, and ethanamine (reactions 16−18), exhibits larger errors for the bond separation reactions of *O*-methylhydroxylamine, acetaldehyde, and acetaldimine (reactions 19−21). Only MP2 and M06-2X yield enthalpies for isodesmic reaction 20 within 0.5 kcal mol^{-1} of the CBS-QB3 benchmark.

These results raise an important question regarding the metrics by which the performance of DFT functionals should be assessed. We have provided examples where functionals that perform well for "real-world" reactions (i.e., reactions 1−9), perform poorly for the simple underlying bonding changes (reactions 10−12). This indicates a reliance on error cancellation that could prove to be troublesome when seeking a reliable computational approach for a given problem. From a pragmatic perspective, such functionals are acceptable because they appear to excel in many applications that are of interest to organic chemists. The failure of these functionals to adequately describe simple changes in bonding that underlie all bond-forming transformations is unnerving. Despite recent advances in DFT functionals, many currently available functionals still sometimes achieve accurate results through the cancellation of sizable errors, not by accurately describing the underlying transformations. Presumably, future theoretical developments will yield DFT functionals that consistently perform well when applied to both complex organic reactions and the underlying bond conversions. Ensuring that new DFT functionals perform well for the simplest chemically meaningful transformations that underlie all bond-forming reactions (e.g., reactions 10−12 and 16−21) should yield robust functionals suitable for organic applications.

This approach is in contrast with the recent work of Korth and Grimme,[56] who champion the use of stochastically generated "artificial molecules" to generate unbiased sets for benchmarking DFT. Such challenging benchmark sets will undoubtedly be valuable in the future to test functionals with universal applicability in chemistry. However, the present suggested path seeks the more immediate goal of identifying robust functionals that deliver consistent thermochemistry for organic reactions by accurately describing the simple underlying changes in bonding and intramolecular effects. Despite shortcomings of currently available functionals, the satisfactory performance of some DFT functionals for the aldol, Mannich, and α-aminoxylation reactions combined with recent progress in functional development[19,26,28] engenders confidence in the application of DFT to the analysis and design of organocatalysts.

Acknowledgment. This work was supported by the National Science Foundation (CHE-0548209). S.E.W. was also supported by an NIH NRSA Postdoctoral Fellowship (NIH-1F32GM082114). A.M. was supported by a predoctoral fellowship of the regional government of the Principado de Asturias. Fernando R. Clemente is thanked for fruitful discussions in the early stages of this work. Computer time was partially provided by the UCLA Institute for Digital Research and Education (IDRE).

Supporting Information Available: Absolute energies, comparison of 6-31+G(d,p) and 6-311+G(2df,2p) results, and Cartesian coordinates. This material is available free of charge via the Internet at http://pubs.acs.org.

References and Notes

(1) (a) Dalko, P. I.; Moisan, L. *Angew. Chem., Int. Ed.* **2001**, *40*, 3726–3748. Dalko, P. I.; Moisan, L. *Angew. Chem., Int. Ed.* **2004**, *43*, 5138–5175. (b) Pellisier, H. *Tetrahedron* **2007**, *63*, 9267–9331. (c) Melchiorre, P.; Marigo, M.; Carlone, A.; Bartoli, G. *Angew. Chem., Int. Ed.* **2008**, *47*, 6138–6171. (d) MacMillan, D. W. C. *Nature* **2008**, *455*, 304–308.

(2) List, B.; Lerner, R. A.; Barbas, C. F., III. *J. Am. Chem. Soc.* **2000**, *122*, 2395–2396.

(3) List, B. *J. Am. Chem. Soc.* **2000**, *122*, 9336–9337.

(4) Cordova, A.; Sunden, H.; Bogevig, A.; Johansson, M.; Himo, F. *Chem. Eur. J.* **2004**, *10*, 3673–3684.

(5) List, B. *Tetrahedron* **2002**, *58*, 5573–5590.

(6) Jiang, L.; Althoff, E. A.; Clemente, F. R.; Doyle, L.; Röthlisberger, D.; Zanghellini, A.; Gallaher, J. L.; Betker, J.; Tanaka, F.; Barbas, C. F., III.; Hilvert, D.; Houk, K. N.; Stoddart, B. L.; Baker, D. *Science* **2008**, *319*, 1387–1391.

(7) Bahmanyar, S.; Houk, K. N. *J. Am. Chem. Soc.* **2001**, *123*, 11273–11283.

(8) Bahmanyar, S.; Houk, K. N. *J. Am. Chem. Soc.* **2001**, *123*, 12911–12912.

(9) Rankin, K. R.; Gauld, J. W.; Boyd, R. J. *J. Phys. Chem. A* **2002**, *106*, 5155–5159.

(10) (a) Bahmanyar, S.; Houk, K. N.; Martin, H. J.; List, B. *J. Am. Chem. Soc.* **2003**, *125*, 2475–2479. (b) Clemente, F. R.; Houk, K. N. *Angew. Chem., Int. Ed.* **2004**, *43*, 5766–5768.

(11) (a) Tang, Z.; Jiang, F.; Yu, L.-T.; Cui, X.; Gong, L.-Z.; Mi, A.-Q.; Jiang, Y.-Z.; Wu, Y.-D. *J. Am. Chem. Soc.* **2003**, *125*, 5262–5263. (b) Cheong, P. H.-Y.; Houk, K. N. *Synthesis* **2005**, *9*, 1533–1537. (c) Mitsumori, S.; Zhang, H.; Cheong, P. H.-Y.; Houk, K. N.; Tanaka, F.; Barbas, C. F., III. *J. Am. Chem. Soc.* **2006**, *128*, 1040–1041. (d) Shinisha, C. B.; Sunoj, R. B. *Org. Biomol. Chem.* **2007**, *5*, 1287–1294.

(12) Houk, K. N.; Cheong, P. H.-Y. *Nature* **2008**, *455*, 309–313.

(13) Hajos, Z. G.; Parrish, D. R. *J. Org. Chem.* **1974**, *39*, 1615–1621.

(14) *Computational Thermochemistry: Prediction and Estimation of Molecular Thermodynamics*; Irikura, K. K.; Frurip, D. J., Eds.; American Chemical Society: Washington, D. C., 1998.

(15) (a) Allen, W. D.; East, A. L. L.; Császár, A. G. In *Structures and Conformations of Non-Rigid Molecules*; Laane, J., Dakkouri, M., van der Veken, B., Oberhammer, H., Eds.; Kluwer: Dordrecht, The Netherlands, 1993; pp 343−373. (b) East, A. L. L.; Allen, W. D. *J. Chem. Phys.* **1993**, *99*, 4638–4650. (c) Tajti, A.; Szalay, P. G.; Császár, A. G.; Kállay, M.; Gauss, J.; Valeev, E. F.; Flowers, B. A.; Vázquez, J.; Stanton, J. F. *J. Chem. Phys.* **2004**, *121*, 11599–11613. (d) Martin, J. M. L. In *Annual Reports in Computational Chemistry*; Elsevier: Amsterdam, 2005; Vol. 1, pp 31−43. (e) Karton, A.; Rabinovich, E.; Martin, J. M. L.; Ruscic, B. *J. Chem. Phys.* **2006**, *125*, 144108.

(16) (a) Koch, W.; Holthausen, M. C. *A Chemist's Guide to Density Functional Theory*; Wiley-VCH: Weinheim, Germany, 2001. (b) Curtiss, L. A.; Raghavachari, K.; Redfern, P. C.; Pople, J. A. *J. Chem. Phys.* **1997**, *106*, 1063–1079.

(17) (a) Cioslowski, J. *Quantum Mechanical Prediction of Thermochemical Data*; Kluwer: Dordrecht, The Netherlands, 2001. (b) Curtiss, L. A.; Raghavachari, K.; Redfern, P. C.; Rassolov, V.; Pople, J. A. *J. Chem. Phys.* **1998**, *109*, 7764–7776. (c) Lynch, B. J.; Truhlar, D. G. *J. Phys. Chem. A* **2003**, *107*, 8996–8999. (d) Zhao, Y.; Gonzales-Gargia, N.; Truhlar, D. G. *J. Phys. Chem. A* **2005**, *109*, 2012–2126. (e) Jurečka, P.; Šponer, J.; Ěerney, J.; Hobza, P. *Phys. Chem. Chem. Phys.* **2006**, *8*, 1985–1993.

(18) Grimme, S.; Steinmetz, M.; Korth, M. *J. Org. Chem.* **2007**, *72*, 2118–2126.

(19) Johnson, E. R.; Mori-Sanchez, P.; Cohen, A. J.; Yang, W. *J. Chem. Phys.* **2008**, *129*, 204112.

(20) (a) Redfern, P. C.; Zapol, P.; Curtiss, L. A.; Raghavachari, K. *J. Phys. Chem. A* **2000**, *104*, 5850–5854. (b) Woodcock, H. L.; Schaefer, H. F.; Schreiner, P. R. *J. Phys. Chem. A* **2002**, *106*, 11923–11931. (c) Leach, A. G.; Goldstein, E.; Houk, K. N. *J. Am. Chem. Soc.* **2003**, *125*, 8330–8339. (d) Bachrach, S. M.; Gilbert, T. M. *J. Org. Chem.* **2004**, *69*, 6357–6364. (e) Check, C. E.; Gilbert, T. M. *J. Org. Chem.* **2005**, *70*, 9828–9834. (f) Schreiner, P. R.; Fokin, A. A.; Pascal, R. A., Jr.; de Meijere, A. *Org. Lett.* **2006**, *8*, 3635–3638. (g) Zhao, Y.; Truhlar, D. G. *Org. Lett.* **2006**, *8*, 5753–5755. (h) Schreiner, P. R. *Angew. Chem., Int. Ed.* **2007**, *46*, 4217–4219. (i) Brittain, D. R. B.; Lin, C. Y.; Gilbert, A. T. B.; Izgorodina, E. I.; Gill, P. M. W.; Coote, M. L. *Phys. Chem. Chem. Phys.* **2009**, *11*, 1138–1142.

(21) (a) Wodrich, M. D.; Corminboeuf, C.; Schleyer, P. v. R. *Org. Lett.* **2006**, *8*, 3631–3634. (b) Wodrich, M. D.; Wannere, C. S.; Mo, Y.; Jarowski, P. D.; Houk, K. N.; Schleyer, P. V. *Chem. Eur. J.* **2007**, *13*, 7731–7744.

(22) Grimme, S. *Angew. Chem., Int. Ed.* **2006**, *45*, 4460–4464.

(23) Pieniazek, S. N.; Clemente, F. R.; Houk, K. N. *Angew. Chem., Int. Ed.* **2008**, *47*, 7746–7749.

(24) (a) Ess, D. H.; Houk, K. N. *J. Phys. Chem. A* **2005**, *109*, 9542–9553. (b) Guner, V.; Khuong, K. S.; Leach, A. G.; Lee, P. S.; Bartberger, M. D.; Houk, K. N. *J. Phys. Chem. A* **2003**, *107*, 11445–11459.

(25) Wodrich, M. D.; Cominboeuf, C.; Schreiner, P. R.; Fokin, A. A.; Schleyer, P. v. R. *Org. Lett.* **2007**, *9*, 1851–1854.

(26) Cohen, A. J.; Mori-Sanchez, P.; Yang, W. *Science* **2008**, *321*, 792–794.

(27) Csonka, G. I.; Ruzsinszky, A.; Perdew, J. P.; Grimme, S. *J. Chem. Theory Comput.* **2008**, *4*, 888–891.

(28) (a) Mori-Sanchez, P.; Cohen, A. J.; Yang, W. *J. Chem. Phys.* **2006**, *125*, 201102. (b) Cohen, A. J.; Mori-Sanchez, P.; Yang, W. *Phys. Rev. B* **2008**, *77*, 115123. (c) Mori-Sanchez, P.; Cohen, A. J.; Yang, W. *Phys. Rev. Lett.* **2008**, *100*, 146401.

(29) Zhang, Y.; Yang, W. *J. Chem. Phys.* **1998**, *109*, 2604–2608.

(30) (a) Montgomery, J. A., Jr.; Frisch, M. J.; Ochterski, J. W.; Petersson, G. A. *J. Chem. Phys.* **1999**, *110*, 2822–2827. (b) Montgomery, J. A., Jr.; Frisch, M. J.; Ochterski, J. W.; Petersson, G. A. *J. Chem. Phys.* **2000**, *112*, 6532–6542.

(31) Ochterski, J. W.; Petersson, G. A.; Montgomery, J. A., Jr. *J. Chem. Phys.* **1996**, *104*, 2598–2619.

(32) (a) Zhao, Y.; Tishchenko, O.; Gour, J. R.; Lutz, J. J.; Piecuch, P.; Truhlar, D. G. *J. Phys. Chem. A* **2009**, *113*, 5786–5799. (b) Wheeler, S. E.; Ess, D. H.; Houk, K. N. *J. Phys. Chem. A* **2008**, *112*, 1798–1807.

(33) Curtiss, L. A.; Raghavachari, K.; Redfern, P. C.; Rassolov, V.; Pople, J. A. *J. Chem. Phys.* **1998**, *109*, 7764–7776.

(34) Becke, A. D. *J. Chem. Phys.* **1993**, *98*, 5648–5652.

(35) Lee, C.; Yang, W.; Parr, R. G. *Phys. Rev. B* **1988**, *37*, 785–789.

(36) (a) Burke, K.; Perdew, J. P.; Wang, Y. In *Electronic Density Functional Theory: Recent Progress and New Directions*; Dobson, J. F., Vignale, G., Das, M. P., Eds.; Plenum: New York, 1998. (b) Perdew, J. P. In *Electronic Structure of Solids*; Ziesche, P., Eschrig, H., Eds.; Akademie: Berlin, 1991; p 11. (c) Perdew, J. P.; Chevary, J. A.; Vosko, S. H.; Jackson, K. A.; Pederson, M. R.; Singh, D. J.; Fiolhais, C. *Phys. Rev. B* **1992**, *46*, 6671–6687.

(37) Becke, A. D. *J. Chem. Phys.* **1996**, *104*, 1040.

(38) (a) Adamo, C.; Barone, V. *J. Chem. Phys.* **1998**, *108*, 664–67. (b) Adamo, C.; Barone, V. *Chem. Phys. Lett.* **1997**, *274*, 242–250.

(39) (a) Perdew, J. P.; Burke, K.; Ernzerhof, M. *Phys. Rev. Lett.* **1996**, *77*, 3865–3868. (b) Perdew, J. P.; Burke, K.; Ernzerhof, M. *Phys. Rev. Lett.* **1997**, *78*, 1396–1396.

(40) Zhao, Y.; Truhlar, D. G. *Theor. Chem. Acc.* **2008**, *120*, 215–241.

(41) Grimme, S. *J. Chem. Phys.* **2003**, *118*, 9095–9102.

(42) Dunning, T. H., Jr. *J. Chem. Phys.* **1989**, *90*, 1007–1023.

(43) Schwabe, T.; Grimme, S. *Acc. Chem. Res.* **2008**, *41*, 569–579.

(44) (a) Bylaska, E. J.; de Jong, W. A.; Govind, N.; Kowalski, K.; Straatsma, T. P.; Valiev, M.; Wang, D.; Aprà, E.; Windus, T. L.; Hammond, J.; Nichols, P.; Hirata, S.; Hackler, M. T.; Zhao, Y.; Fan, P.-D.; Harrison, R. J.; Dupuis, M.; Smith, D. M. A.; Nieplocha, J.; Tipparaju, V.; Krishnan, M.; Wu, Q.; Van Voorhis, T.; Auer, A. A.; Nooijen, M.; Brown, E.; Cisneros, G.; Fann, G. I.; Fruchtl, H.; Garza, J.; Hirao, K.; Kendall, R.; Nichols, J. A.; Tsemekhman, K.; Wolinski, K.; Anchell, J.; Bernholdt, D.; Borowski, P.; Clark, T.; Clerc, D.; Dachsel, H.; Deegan, M.; Dyall, K.; Elwood, D.; Glendening, E.; Gutowski, M.; Hess, A.; Jaffe, J.; Johnson, B.; Ju, J.; Kobayashi, R.; Kutteh, R.; Lin, Z.; Littlefield, R.; Long, X.; Meng, B.; Nakajima, T.; Niu, S.; Pollack, L.; Rosing, M.; Sandrone, G.; Stave, M.; Taylor, H.; Thomas, G.; van Lenthe, J.; Wong, A.; Zhang, Z. *NWChem: A Computational Chemistry Package for Parallel Computers*, version 5.1; Pacific Northwest National Laboratory: Richland, Washington, 2007. (b) Kendall, R. A.; Apra, E.; Bernholdt, D. E.; Bylaska, E. J.; Dupuis, M.; Fann, G. I.; Harrison, R. J.; Ju, J.; Nichols, J. A.; Nieplocha, J.; Straatsma, T. P.; Windus, T. L.; Wong, A. T. *Comput. Phys. Commun.* **2000**, *128*, 260–283.

(45) Frisch, M. J.; Trucks, G. W.; Schlegel, H. B.; Scuseria, G. E.; Robb, M. A.; Cheeseman, J. R.; Montgomery, J. A., Jr.; Vreven, T.; Kudin, K. N.; Burant, J. C.; Millam, J. M.; Iyengar, S. S.; Tomasi, J.; Barone, V.; Mennucci, B.; Cossi, M.; Scalmani, G.; Rega, N.; Petersson, G. A.; Nakatsuji, H.; Hada, M.; Ehara, M.; Toyota, K.; Fukuda, R.; Hasegawa, J.; Ishida, M.; Nakajima, T.; Honda, Y.; Kitao, O.; Nakai, H.; Klene, M.; Li, X.; Knox, J. E.; Hratchian, H. P.; Cross, J. B.; Bakken, V.; Adamo, C.; Jaramillo, J.; Gomperts, R.; Stratmann, R. E.; Yazyev, O.; Austin, A. J.; Cammi, R.; Pomelli, C.; Ochterski, J. W.; Ayala, P. Y.; Morokuma, K.; Voth, G. A.; Salvador, P.; Dannenberg, J. J.; Zakrzewski, V. G.; Dapprich, S.; Daniels, A. D.; Strain, M. C.; Farkas, O.; Malick, D. K.; Rabuck, A. D.; Raghavachari, K.; Foresman, J. B.; Ortiz, J. V.; Cui, Q.; Baboul, A. G.; Clifford, S.; Cioslowski, J.; Stefanov, B. B.; Liu, G.; Liashenko, A.; Piskorz, P.; Komaromi, I.; Martin, R. L.; Fox, D. J.; Keith, T.; Al-Laham, M. A.; Peng, C. Y.; Nanayakkara, A.; Challacombe, M.; Gill, P. M. W.; Johnson, B.; Chen, W.; Wong, M. W.; Gonzalez, C.; Pople, J. A. *Gaussian 03*, revision C.02; Gaussian, Inc.: Wallingford, CT, 2004.

(46) Experimental values are computed form NIST (http://webbook.nist.gov/chemistry) ΔH_f at 298 K and corrected to 0 K using B3LYP/6-31+G(d,p) thermal energy corrections.

(47) Maple, S. R.; Allerhand, A. *J. Am. Chem. Soc.* **1987**, *109*, 6609–6614.

(48) Hehre, W. J.; Radom, L.; Schleyer, P. v. R.; Pople, J. A. *Ab Init o Molecular Orbital Theory*; Wiley-Interscience: New York, 1986.

(49) (a) Hehre, W. J.; Ditchfield, R.; Radom, L.; Pople, J. A. *J. Am. Chem. Soc.* **1970**, *92*, 4796–4801. (b) Radom, L.; Hehre, W. J.; Pople, J. A. *J. Am. Chem. Soc.* **1971**, *93*, 289–300.

(50) (a) George, P.; Trachtman, M.; Bock, C. W.; Brett, A. M. *Theor. Chem. Acc.* **1975**, *38*, 121–129. (b) George, P.; Trachtman, M.; Bock, C. W.; Brett, A. M. *J. Chem. Soc., Perkin Trans. 2* **1976**, 1222–1227.

(51) Wheeler, S. E.; Houk, K. N.; Schleyer, P. v. R.; Allen, W. D. *J. Am. Chem. Soc.* **2009**, *131*, 2547–2560.

(52) Hess, B. A., Jr.; Schaad, L. J. *J. Am. Chem. Soc.* **1983**, *105*, 7500–7505.

(53) Clearly, the $CHO(CH_2)CH(OH)$ fragment present in reaction 1 (Scheme 1) is not equivalent to propane. However, in the context of isodesmic reactions, in which only formal bond types matter, these two three-atom fragments are equivalent in having two CC single bonds. Therefore, when we refer to propane-like or ethanol-like interactions, we are referring to three-atom fragments with the same formal bond types as these simple species, irrespective of hybridization of the termal atoms.

(54) Raghavachari, K.; Stefanov, B. B.; Curtiss, L. A. *J. Chem. Phys.* **1997**, *106*, 6764–6767.

(55) (a) Curtiss, L. A.; Raghavachari, K.; Redfern, P. C.; Pople, J. A. *J. Chem. Phys.* **2000**, *112*, 7374–7383. (b) Cioslowski, J.; Schimeczek, M.; Liu, G.; Stoyanov, V. *J. Chem. Phys.* **2000**, *113*, 9377–9389. (c) Winget, P.; Clarke, T. *J. Comput. Chem.* **2004**, *25*, 725–733. (d) Goumans, T. P. M.; Ehlers, A. W.; Lammertsma, K.; Würthwein, E.-U.; Grimme, S. *Chem. Eur. J.* **2004**, *10*, 6468–6475.

(56) Korth, M.; Grimme, S. *J. Chem. Theory Comput.* **2009**, *5*, 993–1003.

JP9058565